

Space-charge mechanism of aging in ferroelectrics: An analytically solvable two-dimensional model

Yuri A. Genenko*

Institute of Materials Science, Darmstadt University of Technology, Petersenstrasse 23, 64287 Darmstadt, Germany

(Received 5 July 2008; revised manuscript received 17 October 2008; published 9 December 2008)

A mechanism of point defect migration triggered by local depolarization fields is shown to explain some still inexplicable features of aging in acceptor-doped ferroelectrics. A drift-diffusion model of the coupled charged defect transport and electrostatic field relaxation within a two-dimensional domain configuration is treated numerically and analytically. Numerical results are given for the emerging internal bias field of about 1 kV/mm which levels off at dopant concentrations well below 1 mol %; the fact, long ago known experimentally but still not explained. For higher defect concentrations a closed solution of the model equations in the drift approximation as well as an explicit formula for the internal bias field is derived revealing the plausible time, temperature, and concentration dependencies of aging. The results are compared to those due to the mechanism of orientational reordering of defect dipoles.

DOI: [10.1103/PhysRevB.78.214103](https://doi.org/10.1103/PhysRevB.78.214103)

PACS number(s): 77.80.Dj, 61.72.jd, 77.80.Fm, 77.84.Dy

I. INTRODUCTION

The phenomenon of gradual change in physical properties with time, called aging, is for a long time known feature of ferroelectrics, especially when acceptor doped.^{1–13} Aging reveals itself in quasilogarithmic decrease in the dielectric constant with time,^{1,4} reduction in domain-wall mobility leading to stabilization in the aged domain structure,² altered shape of polarization loops in both poled and unpoled aged samples,^{3,5,6,10–13} and related indications. A characteristic aging time, τ , a clamping pressure on the domain walls, P_{cl} , and an internal bias field, E_{ib} , were introduced as parameters quantifying aging.^{5,6}

In the past three decades several concepts were developed^{14,15} to explain the aging phenomena in terms of domain splitting,² space-charge formation,^{3,4} electronic charge trapping at domain boundaries,^{9,10} ionic drift,^{13,16–18} or reorientation of defect dipoles.^{7,8,11,12} The latter concept based on the widely recognized mechanism of gradual orientation of defect dipoles formed by the charged acceptor defects and oxygen vacancies has suggested probably most successful quantitative explanation of many features relevant to aging and fatigue in ferroelectrics, particularly, plausible time and temperature dependencies of E_{ib} . The presence of defect dipoles and their orientation along the polarization direction seem to have been confirmed recently by electron paramagnetic resonance and density functional calculations.^{19,20} Nevertheless, some long-standing questions remain open, most pronounced among them the dependence of τ and E_{ib} on the defect concentration.^{5,6} The individual cage motion of an oxygen vacancy around an acceptor defect is insensitive to the presence of other defect dipoles in the dipole reorientation model.^{7,8} Thus, τ is expected to be independent of the acceptor concentration. Similarly, independent contributions of different defect dipoles to the clamping pressure in this model have to result in E_{ib} directly proportional to the concentration. However, the experimentally observed saturation of E_{ib} at medium concentrations <1 mol % as well as distinct concentration dependence of τ (Refs. 5–7) provides indications of some collective mechanism of aging.

In this paper, therefore, we prove an alternative space-charge mechanism to explain the above-mentioned features of aging. It may also be related to the self-polarization phenomenon and internal field-induced migratory polarization observed in thin ferroelectric films.^{10,21} Recently, a model quantifying the space-charge mechanism was advanced^{22–24} which shows that the clamping pressure $P_{cl} \approx 1$ MPa and the field $E_{ib} \approx 1$ kV/mm comparable with experiments can result from the formation of space-charge zones near charged domain boundaries assuming small but finite mobility of charged defects. Aging was studied first for low defect concentrations about 0.01 mol %, ^{22,23} and the effect of anisotropy was considered.²⁴ Here we apply the isotropic two-dimensional (2D) version of this model²³ studying the aging of unpoled ferroelectrics for a wide range of acceptor concentrations and present numerical and analytical results on temperature, concentration, and time dependencies of E_{ib} . Gradual change in material properties under the effect of the external dc or ac electric field, e.g., fatigue phenomenon, is not considered at this stage.

II. MODEL OF A FERROELECTRIC GRAIN

Main assumptions of the model²³ used here are: (a) availability of mobile charged defects in amount sufficient to substantially compensate the bound charge at the domain boundaries and (b) presence of strong local depolarization fields in the unpoled ferroelectric material.

Let us consider assumption (a). The conductivity of perovskites has been extensively studied during the past two decades.^{25–31} It was established that depending on temperature and partial pressure of oxygen, perovskites may exhibit ionic or electronic conductivity so that the n -type conductivity prevails under reducing conditions and the p type in oxidizing atmospheres.^{25,28,29} The ionic conductivity prevails between the above two areas of electronic conductivity and is clearly dominated by oxygen vacancies. It was shown also that the bulk mobilities of electrons and holes are not activated in BaTiO₃ and exceed the activated mobility of vacancies by many orders of the magnitude. Nevertheless, at at-

mospheric partial oxygen pressure and not very high temperatures, the concentration of electronic carriers remains less than the concentration of vacancies by many orders of the magnitude and is by far not sufficient to compensate the polarization bound charge. Moreover, the bulk concentration of electronic carriers is so small that the corresponding Debye screening length strongly exceeds the typical grain size. This allows one to entirely neglect electronic screening of the local bound charges. The same applies also to ambient electronic carriers in the intergranular space although their concentration may exceed the bulk one by few orders of magnitude.³⁰ The balance between the electronic and ionic species may be substantially changed locally right near the charged domain boundaries because of the electronic band bending by very strong local depolarization fields; however, this possibility depends on the reduction potentials of certain metal dopants.³² In our study we suppose for the simplicity that concentration of electronic carriers is negligible in and outside the ferroelectric grains. The oxygen vacancy concentration is usually fixed by acceptor defects even in the nominally undoped materials since these are as a rule unintentionally acceptor doped.^{28–30} For these reasons, we will assume in the following that only oxygen vacancies participate in charge migration.

Consider now assumption (b). In the perfectly ordered domain system the bound charges at the domain boundaries can be fully compensated resulting in complete suppression of the depolarization fields inside the bulk ferroelectric. Experimental studies show that it is not the case in real disordered systems. Considering the high-resolution images of domain patterns in BaTiO₃ and lead zirconate titanate (PZT) samples by scanning transmission electron microscopy,³³ by bright field transmission electron microscopy,³⁴ and by secondary electron spectroscopy,³⁵ one can observe numerous places where the uncompensated bound charges should emerge and, consequently, local depolarization fields can be present. Three relevant circumstances can be identified, namely, when a domain array (a) ends up in an unpolarized area inside the grain, (b) meets a domain wall of another domain array instead of charged domain faces, and (c) ends up at the grain boundary contacting the wide enough unpolarized intergranular area. To investigate quantitatively the consequences of the presence of uncompensated bound charges in the material the third of the above-mentioned cases, (c), will be representatively studied in the following. Since the depolarization field of a domain array decays exponentially at the distance equal to the domain width a ,^{22,23} it suffices to assume the intergrain spacing larger than a to get the neighbor grains electrically independent. That is why, for studying the effects of local depolarization fields, a model of a single ferroelectric grain surrounded by unpolarized medium may be chosen.

Let us start with a quadratic ferroelectric grain of zero total polarization surrounded by an infinite dielectric medium. We imagine a two-dimensional periodic array of domains in the grain cut by the interfaces with dielectric, $z=0$ and $z=L$, perpendicular to the direction of spontaneous polarization which is along the z direction of a Cartesian coordinate system x , y , and z (Fig. 1). The system is supposed to be uniform in the y direction so that no variable is y dependent.

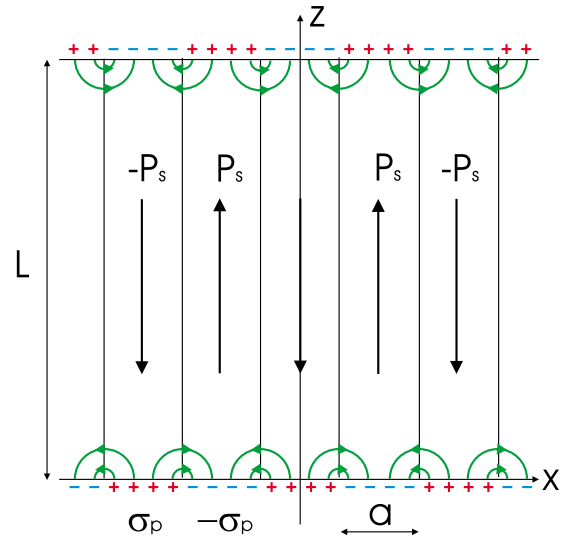


FIG. 1. (Color online) Scheme of a 2D array of 180° domain walls in a quadratic ferroelectric grain occupying the space $|x| < L/2$ and $0 < z < L$. Straight arrows show the direction of the polarization and curved arrows the approximate direction of the local electric field.

If the length of the domains L along the z axis is much larger than their width a along the x axis, which is typically the case in experiments, electric field lines are effectively closed at the same side of the grain. Finite-element simulations of the electric field in the finite domain array shows a virtually periodic field pattern along the x axis everywhere but the very ends of the array.^{22,24} That is why we can consider a periodic domain array infinite along the x axis as a representative model for a finite multidomain grain. This model configuration is well known in the physics of polarized media and was used for the study of equilibrium and dynamic properties of ferromagnetic^{36,37} and ferroelectric³⁸ materials.

Furthermore, since both components of the depolarization field exponentially decrease toward the interior of the grain along the z axis,^{22,23} transport of the charged defects driven by the field is expected to occur in the vicinity of the grain boundaries $z=0$ and $z=L$. Considering charge migration near the interface $z=0$ we can therefore assume the domains to be infinite along the z axis without introducing a substantial error. Apparently, the same process of charge separation occurs at the other grain boundary, $z=L$, too. Calculating the forces exerted upon the domain walls, both ends of the domains must be taken into account.

Hence, to study the depolarization field-induced charge migration it is sufficient to consider the interface $z=0$ between the domain array occupying the ferroelectric half space $z>0$ and the dielectric medium occupying the half space $z<0$. For simplicity, both media are assumed to be isotropic and characterized by the relative dielectric permittivities ϵ_f and ϵ_d , respectively. Due to polarization, the domain faces at $z=0$ are alternatively charged with the bound surface charge density,³⁷

$$\rho_b(x, z) = \sigma_p \delta(z) \sum_{n=-\infty}^{\infty} (-1)^n \theta\left(\frac{a}{2} - an + x\right) \theta\left(\frac{a}{2} + an - x\right), \quad (1)$$

where $\sigma_p = |\mathbf{P}_s|$ is the spontaneous polarization value, $\delta(z)$ and $\theta(x)$ are the Dirac δ function and the Heaviside unit step function, respectively. The choice of the origin in the middle of the positively charged domain face makes the problem also bilaterally symmetrical.

Migration of charge carriers is governed by the drift-diffusion equation which is often used for description of electronic transport in semiconductors:³⁹

$$\partial_t c = -\nabla(\mu c \mathbf{E}) + D \Delta c, \quad (2)$$

where $\mathbf{E}(x, z, t)$ is the local electric field at time t , $c(x, z, t)$ is the concentration of positively charged mobile species, and μ and D are their mobility and diffusivity, respectively. We assume, for simplicity, that the latter two quantities are isotropic and connected by the Einstein relation, $D = \mu kT / q_f$, with k as the Boltzmann constant, T as the absolute temperature, and q_f as the charge of the carriers.

The electric field $\mathbf{E}(x, z, t)$ is determined self-consistently by the charged faces of the domains and the imbalanced charge density in the bulk $\rho(x, z, t) = q_f [c(x, z, t) - c_0]$ through Gauss' law,

$$\nabla \mathbf{E} = \frac{q_f}{\epsilon_f \epsilon_0} (c - c_0), \quad (3)$$

where c_0 is the background concentration of the immobile acceptor defects warranting total electroneutrality and ϵ_0 is the permittivity of vacuum.

For the boundary conditions to the system of Eqs. (2) and (3) we assume usual boundary conditions for the electric field at the interface between the two media³⁷ and chemical isolation of the grain determined by the requirement of vanishing particle current at $z=0$;

$$\mu c E_z - D \partial_z c = 0. \quad (4)$$

Note that the latter condition is not crucial for the present model. Transport of charged species in the dielectric medium (intergranular space) and also through the grain boundary may be additionally included. Here, for simplicity, we consider only redistribution of mobile defects inside the grain.

In the initial state, the system is locally neutral assuming $c(x, z, 0) \equiv c_0$, while the electric field $\mathbf{E}(x, z, 0) \equiv \mathbf{E}^0(\sigma_p | x, z)$ is determined at the beginning solely by the surface charge density [Eq. (1)] and reads, as was calculated in Ref. 23,

$$E_x^0 = \frac{\sigma_p}{\pi \epsilon_0 (\epsilon_f + \epsilon_d)} \ln \left[\frac{\cosh(\pi z/a) + \sin(\pi x/a)}{\cosh(\pi z/a) - \sin(\pi x/a)} \right],$$

$$E_z^0 = \frac{2\sigma_p}{\pi \epsilon_0 (\epsilon_f + \epsilon_d)} \arctan \left[\frac{\cos(\pi x/a)}{\sinh(\pi z/a)} \right]. \quad (5)$$

The latter equations together with boundary conditions and Eqs. (2) and (3) complete the formulation of the problem which can now be treated numerically.

III. NUMERICAL EVALUATION OF THE INTERNAL BIAS FIELD

Numerical solution of the problem is performed using a simple direct Euler scheme described in Ref. 23. Due to the periodicity and the bilateral symmetry of the task, it is sufficient to consider the charge redistribution within the area $0 < x < a$ containing a single domain wall at plane $x=a/2$. Space and time are discretized. At every time step, the change in the carrier concentration is computed from the previous values of the concentration and the electric field using Eq. (2). Updated values of the field are then calculated using Eq. (3). The evaluation is repeated until convergence is achieved.

As an example, we consider now the aging process in unpoled BaTiO₃ doped with a bivalent acceptor, e.g., Ni, Ca, or Mg. For numerical simulations, the material parameters at temperature 45 °C are taken from Refs. 7 and 40 with the aim to compare results directly with those of the theory of dipole reorientation. Namely, it is assumed that $P_s = 2.7 \times 10^{-1}$ C/m², $\epsilon_f = 200$, and $a = 0.5$ μ m. Positively charged oxygen vacancies are assumed as mobile species with q_f twice the elementary charge and the mobility $\mu = 8.4 \times 10^{-22}$ m²/V s implying activation energy of $E_a = 1.1$ eV.^{26,28,29,31}

Note that for the dielectric permittivity the intrinsic lattice value is taken⁴⁰ since the charge migration occurs at the mesoscopic scale of the domain width. The directly measurable macroscopic permittivity may achieve much higher values due to the large contribution of the domain walls⁴¹ which does not apply in the considered problem. Account of anisotropy of crystalline BaTiO₃ would result in enhancement of the field magnitude by the factor $\sqrt{\epsilon_a/\epsilon_c}$ and in reduction in the field penetration depth by the same factor.^{23,24} where $\epsilon_a = 2180$ and $\epsilon_c = 56$ are the principal values of the permittivity tensor.⁴² Since the electrostatic energy is quadratic in the field this would entail the increase in the values of the clamping pressure and the internal bias field by the factor $\sqrt{\epsilon_a/\epsilon_c} \approx 6$. However, for simplicity and comparability with the results of the dipole reorientation model,^{7,8} we assume here the above introduced isotropic permittivity ϵ_f . For the dielectric medium outside the ferroelectric grain we take the same but nonpolarized material with $\epsilon_d = \epsilon_f$.

The system reveals two typical time scales: the drift time $\tau_\mu = a / \mu E_z^0 \approx 7.8 \times 10^6$ s and the diffusion time $\tau_D = a^2 / D \approx 2.2 \times 10^{10}$ s so that the ratio $\beta = \tau_\mu / \tau_D \approx 3.6 \times 10^{-4}$ characterizes the contribution of diffusion to Eq. (2).²³ Although very small, this contribution cannot be neglected because it influences the structure of space-charge zones and provides compatibility with the boundary condition (4). However, because of very small β , large gradients of concentration arise near the negatively charged face of the domain at $z=0$, $a/2 < x < a$ which make the numerical procedure unstable. Since the parameter β affects nothing but the thickness of the positively charged layer piled up near the negatively charged domain face,²³ we assume in computations $\beta = 5 \times 10^{-2}$ keeping in mind that this may lead to mistakes if the thickness of the space-charge zone in front of the positively charged domain face becomes comparable with βa . Details on the field and concentration profiles and their evolution with time are

exemplary presented in Ref. 23 for low dopant concentrations about $c_0=0.01$ mol %. Here computations are extended over the region from $c_0=0.01$ to 1 mol %.

Having the charge density and the electric field calculated, the time-dependent forces exerted upon domain walls can be evaluated. The loss of domain-wall mobility characteristic of aging results from relaxation of the energy of the electrostatic depolarization field due to piling up of the charged defects at the charged domain faces. Distribution of the energy of this field and of the consequent clamping pressure along the domain wall is very nonuniform, peaking at the domain boundaries.²³ The average clamping pressure preventing the displacement of the domain wall from the energy minimum and the corresponding internal bias field may be estimated as follows.

The thermodynamic force exerted upon the domain wall can be defined as the derivative of the energy of the electrostatic field on the domain-wall displacement. This derivative may be roughly estimated from the difference between the energy of the initial state of the system displayed in Fig. 1 and the fully polarized state achieved by the virtual displacement of domain walls over the distance of $a/2$.

The energy of the electrostatic field per one half of the domain length reads

$$W[\mathbf{E}] = \frac{1}{2} \varepsilon_0 \varepsilon_f \int_{-\infty}^{L/2} dz \int_0^a dx \mathbf{E}^2, \quad (6)$$

while the other half of the domain at $z > L/2$ contributes to the same amount of the energy for symmetry reasons. In the virgin state of the grain, the depolarization field is represented by Eq. (5), and the energy of this field per one period of the structure is given by the well-known formula,^{36–38}

$$W[\mathbf{E}^0(\sigma_p)] = 0.85 \frac{\sigma_p^2 a^2}{4\pi \varepsilon_0 \varepsilon_f}. \quad (7)$$

In the course of aging, the electric field transforms to $\mathbf{E} = \mathbf{E}^0(\sigma_p) + \Delta\mathbf{E}$, where $\Delta\mathbf{E}$ is the contribution to the field due to the charge-carrier migration. The aged state of the structure in Fig. 1 serves as the initial state with the energy $W[\mathbf{E}]$ in the clamping force calculation.

Consider now the virtual pairwise displacement of the domain walls to each other until they meet which leads to the full polarization of the system in the positive z direction. The resulting uniform bound charge at the grain boundaries at $z=0$ and $z=L$ generates then the uniform depolarization field $\mathbf{E}_d = (0, 0, -P_s/\varepsilon_0 \varepsilon_f)$, $0 < z < L$, so that the total electric field becomes equal to $\mathbf{E}_f = \mathbf{E}_d + \Delta\mathbf{E}$. The energy of the electrostatic field in this state amounts to $W[\mathbf{E}_f]$. The clamping pressure on the domain walls related to aging is provided by the time-dependent part of the energy difference $W[\mathbf{E}_f] - W[\mathbf{E}]$, namely,

$$\Delta W_{cl} = \varepsilon_0 \varepsilon_f \int_{-\infty}^{L/2} dz \int_0^a dx (\mathbf{E}_d - \mathbf{E}^0) \Delta\mathbf{E}. \quad (8)$$

Calculating here the energy gain near the domain boundary at $z=0$ the integration limit $L/2$ can be extended to infinity

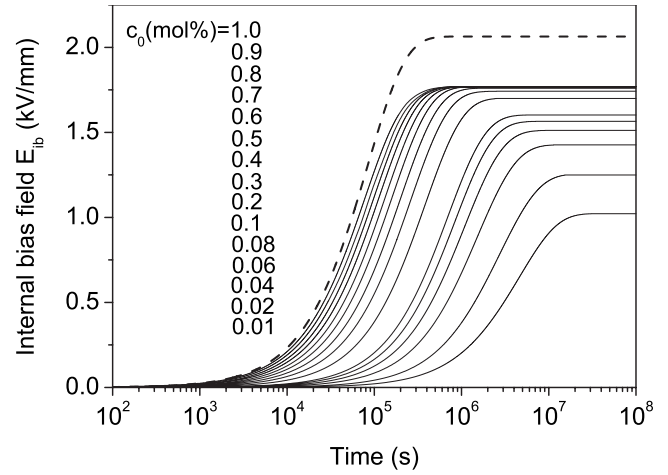


FIG. 2. E_{ib} as a function of time for variable acceptor concentration c_0 which increases monotonically from the lower to the upper curve (solid lines). The dashed line presents the theoretical limit of high c_0 (see text).

because of the exponentially fast decrease in the fields \mathbf{E}^0 and $\Delta\mathbf{E}$ in both directions of z axis.

Finally, the internal bias field in the z direction can be evaluated comparing the force $2P_s \mathcal{E}L$ (Ref. 43) exerted upon the domain wall by an external field \mathcal{E} with the clamping force $2\Delta W_{cl}/(a/2)$ accounting now for both domain boundaries. This results in the estimation,

$$E_{ib} \simeq \frac{2}{aLP_s} \Delta W_{cl}. \quad (9)$$

Evaluation of the time-dependent field E_{ib} assuming the typical length of the domain wall $L=20a$ is shown in Fig. 2 for different dopant concentrations. All the curves demonstrate saturation of E_{ib} after a some characteristic (aging) time τ which decreases with the growing concentration. The final, equilibrium value of E_{ib} first increases with the concentration but then levels off well below $c_0 \approx 1.0$ mol % as is seen in Fig. 3. The inversed aging time τ^{-1} rises almost linearly with the increasing doping in the whole range of studied concentrations. Saturating dependence of E_{ib} on c_0 is clearly seen in experiments on the acceptor-doped PZT (Refs. 5 and 6); indications of both above described E_{ib} and τ dependencies are observable on the acceptor-doped barium titanate too.⁷

Saturation of E_{ib} as well as decreasing of aging time with growing concentration c_0 has a simple physical reason. The depth Δ of the space-charge area emerging near the positively charged domain boundary is defined by the amount of carriers needed to fully compensate the surface bound charge and is of the order of $\sigma_p/(q_f c_0)$. For the concentration of $c_0=1$ mol % it is about 5.4 nm which is 2 orders of the magnitude smaller than the domain width a . This means that at so high concentrations, the electrostatic depolarization field is compensated virtually in the whole specimen volume due to the charge migration so that the maximum possible energy gain and, consequently, the maximum magnitude of E_{ib} is achieved which is concentration independent. At

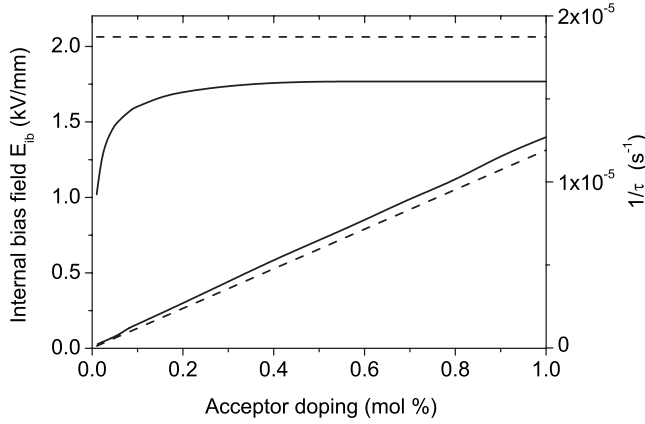


FIG. 3. Saturated value of E_{ib} (two upper curves) and inverse aging time (two lower curves), τ^{-1} , determined from the inflection point of plots in Fig. 2, are presented as functions of acceptor concentration c_0 by solid lines. Respective theoretical values derived in the limit of high c_0 (see text) are shown by dashed lines.

smaller concentrations, especially below $c_0=0.1$ mol %, the extended space-charge zone exists near the positively charged domain face where the depolarization field is still present.²³ This makes the field suppression incomplete so that the energy gain and, consequently, E_{ib} is not maximum and increases with the concentration. The characteristic time of aging is determined, in turn, by the distance Δ the charge carriers have to cover and is obviously proportional to $\Delta/\mu E_z^0 \sim 1/c_0$. The delineated dependencies of both E_{ib} and τ are clearly seen in Figs. 2 and 3.

IV. ANALYTICAL SOLUTION FOR MEDIUM AND HIGH DEFECT CONCENTRATIONS

If the vacancy concentration is high enough in the sense of charge compensation mechanism discussed in Sec. III, the problem may be substantially simplified by neglecting the diffusion contribution relevant only within the thin space-charge zone. Then Eq. (2) considered in the drift approximation reads

$$\partial_t c = -\nabla(\mu c \mathbf{E}). \quad (10)$$

The boundary condition (4), where drift was outweighed by diffusion, does not apply anymore. To keep charge balance this condition is substituted by the requirement on the surface charge density $\sigma(x, t)$ which now embraces the space-charge zones and can be obtained by integration of Eq. (10) over an infinitesimal region near the boundary,

$$\partial_t \sigma(x, t) = -q_f \mu c(x, +0, t) E_z(x, +0, t). \quad (11)$$

This assumption implies that the defect concentration remains constant in the bulk resulting in an ansatz,

$$c(x, z, t) = c_0 + \delta(z)\sigma(x, t). \quad (12)$$

Since $E_z(x, +0, t) = \sigma(x, t)/(\epsilon_f + \epsilon_d)$, Eq. (11) leads to an equation for the surface charge density,

$$\partial_t \sigma(x, t) = -\sigma(x, t)/\tau_r, \quad (13)$$

with the Maxwell relaxation time $\tau_r = \epsilon_0(\epsilon_f + \epsilon_d)/\kappa$, where $\kappa = q_f \mu c_0$ is the ionic conductivity of the bulk material. An apparent initial condition for $\sigma(x, t)$ reads $\sigma(x, 0) = \sigma_p \text{sgn}(a/2 - x)$ which provides a solution $\sigma(x, t) = \sigma_s(t) \text{sgn}(a/2 - x)$, with $\sigma_s(t) = \sigma_p \exp(-t/\tau_r)$. The asymptotic condition $\sigma_s(t \rightarrow \infty) = 0$ means full compensation of the bound charge.

With ansatz (12), Eq. (3) becomes homogeneous and is satisfied by the function $\mathbf{E}^0(\sigma_s(t)|x, z)$. The drift Eq. (10) is then self-evident satisfied in the bulk. The part of the field due to charge migration equals consequently $\Delta \mathbf{E} = -\mathbf{E}^0(\sigma_p)[1 - \exp(-t/\tau_r)]$.

Substituting $\Delta \mathbf{E}$ into Eq. (8) one can note that for symmetry reasons, the first term in the brackets does not contribute to the energy. Finally, an explicit formula for the internal bias field follows from Eq. (9):

$$E_{ib}(t) \approx \frac{0.85 a P_s}{\pi L \epsilon_0 \epsilon_f} [1 - \exp(-t/\tau_r)]. \quad (14)$$

Note that neglecting the thickness of the space-charge zone, the saturated (asymptotic) magnitude of E_{ib} achieves the concentration-independent maximum value determined by the electrostatic energy of the stripe domain structure [Eq. (7)]. The aging time τ is represented by the Maxwell relaxation time τ_r which is, as expected, proportional to $1/c_0$.

The dependence [Eq. (14)] is shown exemplary for the concentration $c_0=1$ mol % on the Fig. 2 (dashed line). It describes well an increase in the corresponding computed curve for E_{ib} below the aging time but levels off at the magnitude approximately 15% larger than the computed value. We interpret this difference as a result of the growing numerical mistake at high concentrations c_0 when the thickness of the space-charge zone becomes of the order of βa as discussed in Sec. III. The Maxwell relaxation time (dashed line) describes well the aging time at all concentrations considered as is shown in Fig. 3.

The field E_{ib} is temperature dependent through the parameters ϵ_f and τ_r of the formula (14). ϵ_f changes strongly when temperature increases toward the ferroelectric transition that is regarded as in Ref. 7. The dependence of τ_r is a more subtle question since, in the considered temperature range, the directly measured total conductivity can be dominated by electron holes²⁹⁻³¹ because of their mobility much higher than the ionic one. However, the density of electronic carriers remains, as was discussed in Sec. II, much lower than that of oxygen vacancies and cannot contribute much to the bound charge compensation. That is why in evaluation of τ_r only the ionic conductivity $\kappa(T) = \kappa_0 \exp(-E_a/kT)$ is included with the activation energy $E_a = 1.1$ eV and $\kappa_0 = 112.8(\Omega \text{ cm})^{-1}$ for $c_0=1$ mol %.²⁹ For these c_0 and E_a , time dependences of E_{ib} by different temperatures are presented in Fig. 4 by solid lines. In fact, the activation energy for oxygen vacancies is not known accurately and usually estimated as $E_a = (1 \pm 0.1)$ eV.^{26,31} Assuming, as in Ref. 8,

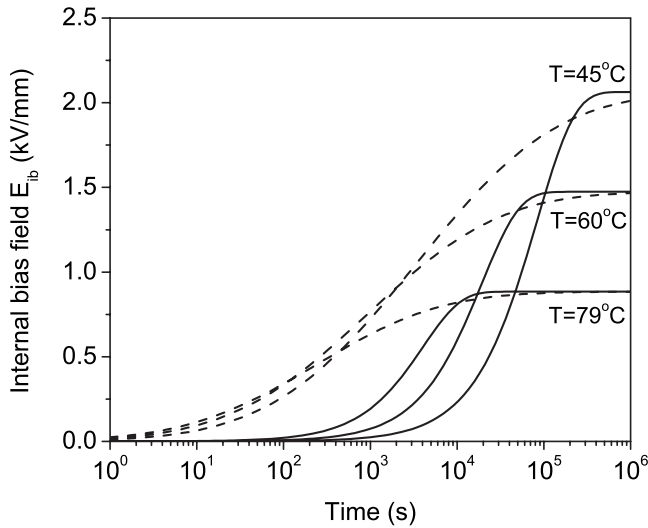


FIG. 4. E_{ib} as a function of time for activation energy $E_a=1.1$ eV, acceptor concentration $c_0=1$ mol % and variable temperature as indicated in the plot (solid lines). E_{ib} averaged over the Gauss distribution of the random energies E_a (dashed lines).

that E_a is a random variable distributed with a Gaussian $\sim \exp[(E_a - \bar{E})^2 / 2s^2]$ using $\bar{E}=1$ eV and $s/\bar{E}=0.1$, E_{ib} can be averaged over this distribution^{8,44} resulting in a quasilogarithmic time dependencies shown by the dashed lines for different temperatures in Fig. 4.

Theoretical curves in Fig. 4 represent satisfactorily experimental time and temperature dependencies of E_{ib} .^{7,8} Somewhat overestimated value of E_{ib} could be adjusted by the factor a/L which is, in fact, the only fitting parameter in this theory. In the performed calculations it was taken equal to 0.05 but it is, in fact, slightly dependent on the grain size and lies between 0.02 and 0.05.⁴⁵ The parameter a/L may be also used to account for the fact that not every domain array is pinned by the local charges. The domain arrays which perfectly match other domain arrays, compensating bound charges, are stiffly coupled to each other. This means that for L some effective domain length L_{eff} can be taken which may exceed L few times but is hardly larger than the grain size.

The curves in Fig. 4 resemble those in the theory of dipole reorientation^{7,8} although the mechanisms involved are completely different which reveals itself in different dependencies on the doping concentration. Note that the described here space-charge mechanism of domain pattern fixation near domain boundaries does not preclude at all the dipole reorientation mechanism which can still be valid in the bulk of the grain.

V. DISCUSSION AND CONCLUSIONS

The two-dimensional model of depolarization field-induced charge migration has been presented which explains plausibly the time, temperature, and doping dependencies of the internal bias field in aging ferroelectrics. Saturation of this field as well as decrease in the aging time with the increasing dopant concentration is in agreement with experi-

mental observations.⁵⁻⁷ This is in contrast to the theory of defect dipole reorientation^{7,8} based on the picture of individual cage motion of oxygen vacancies which predicts the internal bias field proportional to and the aging time independent of the dopant concentration.

A reasonable question arises: whether account of interaction between defect dipoles could modify the dipole rotation theory so that it explains the concentration dependence properly. This possibility should indeed be carefully studied. It is known, at least, that at high vacancy concentrations, substantial structural changes in the subsystem of vacancies may occur.⁴⁶ This happens, however, at about $c_0=7$ mol %, while the substantial deviations from the linear dependence of E_{ib} on concentration become apparent already at $c_0=0.1$ mol %.^{5,6} Note that doping below 1 mol % is usually considered as very dilute.⁴⁷ On the other hand, one should take into account possible chemical restrictions on solubility of certain acceptors in the bulk of the grains.⁴⁸ In any case, a concentration of about 1 mol % is high enough in the sense of the presented here space-charge mechanism of screening of polarization which allows for good agreement with experiment.⁵⁻⁷

The proposed two-dimensional model of charge migration can be extended to include further features and mechanisms which may influence aging. Note that the change in the 180° domain walls to the 90° walls in the sketch presented in Fig. 1 does not entail strong modification of the results and is reduced solely to the substitution of $\sigma_p=|\mathbf{P}_s|$ by $\sigma_p=|\mathbf{P}_s|/\sqrt{2}$. A more important task is to take into account the possible change in the domain pattern during the charge migration. The metastable domain structure results from the compromise between the energy of the electrostatic depolarization field and the energy of domain walls.^{36,38} The relaxation of the electrostatic energy can trigger the change in the domain pattern including possible creation or disappearance of domain walls at the grain boundaries. This process, in turn, involves the energy contribution of the mechanical stresses which has not been considered in this model as yet. One more idealization of the suggested model is an abrupt change in the polarization at the domain boundaries. Considering space distribution of the polarization within the Ginzburg-Landau approach reveals that characteristic scale at which the polarization gradually changes may become comparable with the domain width, especially when the temperature is not far from the temperature of the phase transition into the paraelectric state.⁴⁹ Including the ferroelastic interaction in the Ginzburg-Landau description may also substantially change the form of the domains providing appearance of the well-known needle-shaped domains.⁵⁰ These all additional features do not preclude, nevertheless, the appearance of strong local depolarization fields which present the crucial element of the actual model of aging due to charged defects migration. Self-consistent analysis of the system evolution with many additional variables presents a very challenging task which may be addressed in the future. At the actual stage, only electrostatic arguments were observed so far which allow, however, comparison with the theory of defect dipole reorientation where only electrostatic contributions were included, too.

ACKNOWLEDGMENTS

Discussions with Nina Balke, Ruediger Eichel, Edwin Garcia, Xin Guo, Hans Kungl, Igor Lukyanchuk, Doru Lupascu, Maxim Morozov, Ralf Mueller, Igor Pronin, Hermann

Rauh, Jurgen Roedel, Don Smyth, Alexander Tagantsev, Reiner Waser, and Vadim Kirillovich Yarmarkin are gratefully acknowledged. This work was supported by the Deutsche Forschungsgemeinschaft through Sonderforschungsbereich 595.

*yugenen@tgm.tu-darmstadt.de

- ¹K. W. Plessner, Proc. Phys. Soc. B **69**, 1261 (1956).
- ²S. Ikegami and I. Ueda, J. Phys. Soc. Jpn. **22**, 725 (1967).
- ³M. Takahashi, Jpn. J. Appl. Phys. **9**, 1236 (1970).
- ⁴H. Thomann, Ferroelectrics **4**, 141 (1972).
- ⁵K. Carl and K. H. Härdtl, Ferroelectrics **17**, 473 (1978).
- ⁶S. Takahashi, Ferroelectrics **41**, 277 (1982).
- ⁷G. Arlt and H. Neumann, Ferroelectrics **87**, 109 (1988).
- ⁸R. Lohkämper, H. Neumann, and G. Arlt, J. Appl. Phys. **68**, 4220 (1990).
- ⁹W. L. Warren, D. Dimos, B. A. Tuttle, G. E. Pike, R. W. Schwartz, P. J. Clews, and D. C. McIntyre, J. Appl. Phys. **77**, 6695 (1995).
- ¹⁰V. P. Afanasjev, A. A. Petrov, I. P. Pronin, E. A. Tarakanov, and E. Ju. Kaptelov and J. Graul, J. Phys.: Condens. Matter **13**, 8755 (2001).
- ¹¹L. X. Zhang and X. Ren, Phys. Rev. B **71**, 174108 (2005).
- ¹²L. X. Zhang and X. Ren, Phys. Rev. B **73**, 094121 (2006).
- ¹³M. I. Morozov and D. Damjanovic, J. Appl. Phys. **104**, 034107 (2008).
- ¹⁴A. K. Tagantsev, I. Stolichnov, E. L. Colla, and N. Setter, J. Appl. Phys. **90**, 1387 (2001).
- ¹⁵M. Dawber, K. M. Rabe, and J. F. Scott, Rev. Mod. Phys. **77**, 1083 (2005).
- ¹⁶H.-J. Hagemann, J. Phys. C **11**, 3333 (1978).
- ¹⁷P. V. Lambeck and G. H. Jonker, J. Phys. Chem. Solids **47**, 453 (1986).
- ¹⁸J. F. Scott, B. Pouligny, K. Dimmler, M. Parris, D. Butler, and S. Eaton, J. Appl. Phys. **62**, 4510 (1987).
- ¹⁹R.-A. Eichel, P. Erhart, P. Träskelin, K. Albe, H. Kungl, and M. J. Hoffmann, Phys. Rev. Lett. **100**, 095504 (2008).
- ²⁰L. X. Zhang, E. Erdem, X. Ren, and R.-A. Eichel, Appl. Phys. Lett. **93**, 202901 (2008).
- ²¹A. L. Kholkin, K. G. Brooks, D. V. Taylor, S. Hiboux, and N. Setter, Integr. Ferroelectr. **22**, 525 (1998).
- ²²D. C. Lupascu, Y. A. Genenko, and N. Balke, J. Am. Ceram. Soc. **89**, 224 (2006).
- ²³Y. A. Genenko and D. C. Lupascu, Phys. Rev. B **75**, 184107 (2007); **76**, 149907(E) (2007).
- ²⁴Y. A. Genenko, N. Balke, and D. C. Lupascu, Ferroelectrics **370**, 196 (2008).
- ²⁵G. M. Choi, H. L. Tuller, and D. Goldschmidt, Phys. Rev. B **34**, 6972 (1986).
- ²⁶R. M. Waser, J. Am. Ceram. Soc. **74**, 1934 (1991).
- ²⁷C. J. Brennan, Integr. Ferroelectr. **7**, 93 (1995).
- ²⁸M. V. Raymond and D. M. Smyth, J. Phys. Chem. Solids **57**, 1507 (1996).
- ²⁹D. M. Smyth, J. Electroceram. **11**, 89 (2003).
- ³⁰X. Guo, C. Pithan, C. Ohly, C. L. Jia, J. Dornseiffer, F.-H. Hae-gel, and R. Waser, Appl. Phys. Lett. **86**, 082110 (2005).
- ³¹C. Ohly, S. Hoffmann-Eifert, X. Guo, J. Schubert, and R. Waser, J. Am. Ceram. Soc. **89**, 2845 (2006).
- ³²P. M. Jones, D. E. Gallardo, and S. Dunn, Chem. Mater. **20**, 5901 (2008).
- ³³A. Schilling, R. M. Bowman, J. M. Gregg, G. Catalan, and J. F. Scott, Appl. Phys. Lett. **89**, 212902 (2006).
- ³⁴L. A. Schmitt, K. A. Schonau, R. Theissmann, H. Fuess, H. Kungl, and M. J. Hoffmann, J. Appl. Phys. **101**, 074107 (2007).
- ³⁵M. U. Farooq, R. Villaurrutia, I. Maclaren, H. Kungl, M. J. Hoffmann, J. J. Fundenberger, and E. Bouzy, J. Microsc. **230**, 445 (2008).
- ³⁶C. Kittel, Phys. Rev. **70**, 965 (1946).
- ³⁷L. D. Landau and E. M. Lifshitz, *Electrodynamics of Continuous Media* (Pergamon, Oxford, 1963).
- ³⁸T. Mitsui and J. Furuichi, Phys. Rev. **90**, 193 (1953).
- ³⁹S. M. Sze, *Physics of Semiconductor Devices* (Wiley, New York, 1969).
- ⁴⁰B. Jaffe, W. R. Cook, Jr., and H. Jaffe, *Piezoelectric Ceramics* (Academic, Marietta, OH, 1971).
- ⁴¹Y. L. Wang, A. K. Tagantsev, D. Damjanovic, and N. Setter, Appl. Phys. Lett. **91**, 062905 (2007).
- ⁴²M. Zgonik, P. Bernasconi, M. Duelli, R. Schlessler, P. Gunter, M. H. Garrett, D. Rytz, Y. Zhu, and X. Wu, Phys. Rev. B **50**, 5941 (1994).
- ⁴³V. N. Nechaev and A. M. Roschupkin, Ferroelectrics **90**, 29 (1989).
- ⁴⁴A. K. Tagantsev, I. Stolichnov, N. Setter, J. S. Cross, and M. Tsukada, Phys. Rev. B **66**, 214109 (2002).
- ⁴⁵M. J. Hoffmann, M. Hammer, A. Endriss, and D. C. Lupascu, Acta Mater. **49**, 1301 (2001).
- ⁴⁶S. Steinsvik, R. Bugge, J. Gjonnes, J. Taftø, and T. Nordby, J. Phys. Chem. Solids **58**, 969 (1997).
- ⁴⁷J. F. Scott and M. Dawber, Appl. Phys. Lett. **76**, 3801 (2000).
- ⁴⁸C. Fetzer, I. Dezsai, S. Lauterbach, H.-J. Kleebe, S. Hummelt, and A. G. Balogh (unpublished).
- ⁴⁹F. De Guerville, M. El Marssi, I. Lukyanchuk, and L. Lahoche, Ferroelectrics **359**, 14 (2007).
- ⁵⁰E. K. H. Salje and Y. Ishibashi, J. Phys.: Condens. Matter **8**, 8477 (1996).